Current Sensorless PV Curve Tracer: A Comparative Study of Signal Processing Techniques

1st Luis Gustavo Teixeira Campos
Departamento de Eng. Elétrica
Universidade Federal de Viçosa
Viçosa, Brazil
luis.campos@ufv.br

2nd Paulo Henrique Souza Ferreira
Departamento de Eng. Elétrica
Universidade Federal de Viçosa
Viçosa, Brazil
paulo.ferreira1@ufv.br

3rd Luis Antônio Gregório Lopes
Departamento de Eng. Elétrica
Universidade Federal de Viçosa
Viçosa, Brazil
luis.a.lopes@ufv.br

4th Ives de Oliveira Furtado
Programa de Pós-Graduação em Eng. Elétrica
Centro Federal de Educação Tecnológica de Minas Gerais
Belo Horizonte, Brazil
ives.furtado@ufv.br

5th Victor Dardengo
Departamento de Eng. Elétrica
Universidade Federal de Viçosa
Viçosa, Brazil
victor.dardengo@ufv.br

6th Heverton Augusto Pereira
Departamento de Eng. Elétrica
Universidade Federal de Viçosa
Viçosa, Brazil
heverton.pereira@ufv.br

***Abstract*—This paper presents a comparative study of signal processing techniques for noise reduction in voltage measurements from a low-cost, current sensorless photovoltaic (PV) curve tracer. The device estimates current indirectly from voltage data using a capacitive load, eliminating the need for a dedicated current sensor and reducing overall system cost. However, this approach increases the impact of noise on current estimation, making effective signal processing essential. Three techniques are evaluated: a digital low-pass filter, polynomial fitting, and a novel method based on fitting the single diode model (SDM) of PV cells. Experimental results using real PV module data demonstrate that while all methods improve current estimation, the SDM-based approach achieves the highest accuracy, as confirmed by statistical metrics. The findings highlight the trade-offs between computational complexity and estimation quality, providing practical guidance for the design of low-cost PV characterization instruments.**

***Index Terms*—Photovoltaic curve tracer, current sensorless, signal processing, single diode model, PV characterization.**

I. Introduction

In recent years, solar energy sources have shown significant growth worldwide. In Brazil, this source represents more than 20% of the installed energy matrix [1], [2]. This growth can be attributed to the reduction in photovoltaic system costs over the past decades. According to historical data from the International Renewable Energy Agency(IRENA), the cost of photovoltaic modules has decreased significantly: from over US$100/W in 1975 to less than US$0.50/W in recent years, representing a cost reduction of over 99% [3], [4]. This trend is also reflected in Brazil, where residential photovoltaic systems had average installation costs of around R$2.80 per watt in the first quarter of 2024 [5]. This price reduction is the result of large investments in new technologies, combined with strong automation in production, economies of scale, and technological improvements, allowing for more competitive manufacturing even in locations with high labor costs [6], [7].

The maintenance of photovoltaic plants is directly linked to the performance of their modules, which is assessed through current-voltage (I-V) characterization using an IV curve tracer (IVCT). This instrument records the voltage and current output of a photovoltaic module, enabling the extraction of key parameters such as short-circuit current (I_{sc}), open-circuit voltage (V_{oc}) and maximum power point (MPP). These parameters are necessary for evaluating module efficiency, diagnosing faults, and planning maintenance activities [8].

I-V curve tracers can be designed using several topologies, most commonly based on electronic loads [9], capacitive loads [10], or resistive loads [11]. Each approach presents distinct advantages and disadvantages.

Devices based on electronic loads, while typically more expensive due to their circuit complexity, offer superior control over the voltage sweep time. In contrast, capacitive load-based tracers provide a reliable, low-cost solution; however, the fixed capacitance value makes the sweep time dependent on the solar irradiance level. Finally, resistive load-based devices can be inexpensive and easily controlled, but achieving high-resolution characterization requires a wide range of resistance values. This requirement can increase the instrument's physical size while still yielding lower resolution compared to the other topologies.

Considering these factors, I-V curve tracers based on capacitive loads are the most prevalent in the market, as they offer a favorable balance between cost and performance. In the pursuit of further cost reduction, additional simplifications

The authors are grateful for the financial support provided by the P&D project ANEEL/CEMIG D0727, CNPq (Conselho Nacional de Desenvolvimento Científico e Tecnológico) - projects 311056/2020-2, 408059/2021-4 and 307172/2022-8 and FAPEMIG (Fundação de Amparo à Pesquisa do Estado de Minas Gerais) - projects APQ-02556-21 and RED-00216-23. In addition, this work was carried out with the support of the CAPES (Coordenação de Aperfeiçoamento de Pessoal de Nível Superior) - Financing Code 001 and Academic Excellence Program (PROEX).

can be implemented. A significant trade-off exists between the cost and the quality of sensors used in these devices, as low-cost current sensors often exhibit poor accuracy.

To address this, some recent designs have adopted a current-sensorless approach, which estimates the current indirectly from voltage measurements [12]. This method eliminates the need for a dedicated current sensor, reducing overall cost but increasing the complexity of post-processing. The accuracy of this approach is highly dependent on the quality of the voltage measurements and the electrical characteristics of the load. Consequently, noise and inaccuracies in the voltage data can significantly degrade the current estimation, making advanced signal processing techniques essential for improving measurement quality.

Aiming to enhance current estimation in sensorless curve tracers, this work evaluates and compares three distinct signal processing techniques for noise reduction in voltage measurements. The comparison includes two widely used techniques and a novel approach proposed by the authors, which is based on the single diode model (SDM) of photovoltaic cells. This paper is organized as follows: Section II describes the low-cost, current-sensorless curve tracer used in this work. Section III presents the signal processing techniques evaluated. Section IV discusses the results obtained, and Section V concludes the paper.

II. The Low-Cost Current Sensorless Curve Tracer

The devices which we refer to as "current sensorless curve tracers," estimate current indirectly by analyzing the voltage response across a capacitor during charging, with the current being calculated using (1).

$$I = C\frac{\Delta V}{\Delta t} \tag{1}$$

Figure 1 (a) shows typical voltage data from the current sensorless curve tracer. Although the data appears clean, the calculated current seen in Figure 1 (b) shows considerable noise. Improving voltage signal conditioning circuit would increase cost, so post-processing techniques are preferred.

The current sensorless curve tracer employed in this work is the Gtracer, a low-cost device developed by the GESEP (Gerência de Especialista de Sistemas Elétricos de Potência) group at the Federal University of Viçosa [10], [13]. Unlike conventional IVCTs that directly measure both voltage and current, this equipment operates based on a capacitive load principle, estimating current indirectly from voltage measurements. The device is self-powered, utilizes an ESP32 microcontroller, and does not require a current sensor. Its operation and data acquisition are managed through a web interface, which allows the users to control the device, monitor measurements, and store the curve trace data.

The Figure 2 (a) shows a photo of the Gtracer equipment and Figure 2 (b) presents a simplified diagram of the circuit implemented in the device.

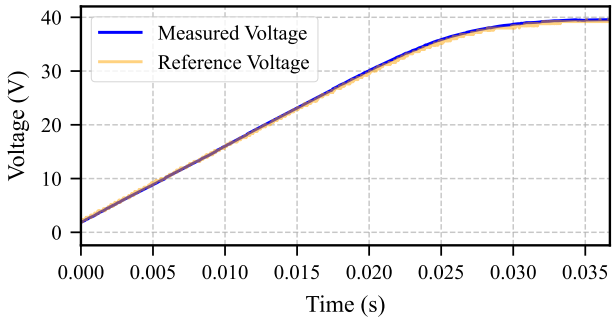

(a) Voltage × Time.

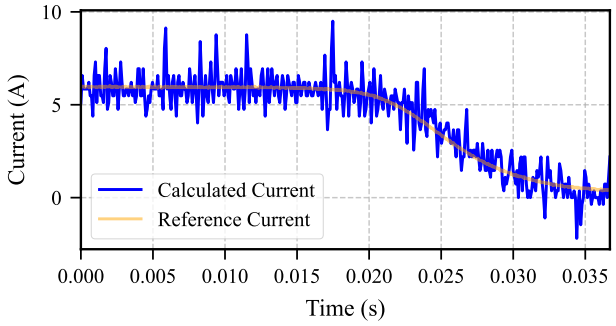

(b) Current × Time.

Fig. 1: (a) Raw voltage data from the curve tracer. (b) Current calculated using the voltage data.

TABLE I: Gtracer Technical Specifications.

Aspect	Specification
Max Voltage	70 V
Max Current	20 A
Capacitor Value	0.0044 F
Data Acquisition	400 voltage samples per trace
Interface	Web-based (Wi-Fi)
Connection	Bluetooth Low Energy (BLE)
Measurement Principle	Capacitive load
Microcontroller	ESP32

III. Signal Processing

A. Low-Pass Filter

The first approach to reduce noise in the signal is the application of a digital low-pass filter, which allows low-frequency components to pass while attenuating high-frequency noise, which may originate from sources such as electromagnetic interference, thermal noise, or other random fluctuations. The low-pass filter is implemented according to the following equation:

$$y[n] = \alpha x[n] + (1-\alpha)y[n-1] \tag{2}$$

where $y[n]$ is the filter output at time n, $x[n]$ is the input signal at time n and α is a constant that determines the cut-off frequency. The parameter α can be adjusted to control the degree of filtering: smaller values result in stronger attenuation

(a) Gtracer equipment.

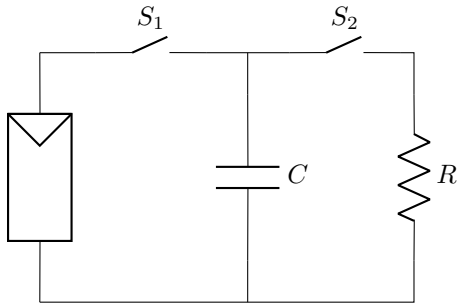

(b) Internal circuit.

Fig. 2: (a) Photo of the Gtracer equipment; (b) Simplified internal circuit diagram.

of high frequencies, while larger values reduce the filtering intensity. The value of α is given by:

$$\alpha = \frac{1}{1 + \frac{2\pi f_c}{f_s}} \tag{3}$$

where f_c is the cut-off frequency and f_s is the sampling frequency. The cut-off frequency defines the point at which the filter begins to attenuate the input signal. Since the voltage signal exhibits an exponential-like behavior and is predominantly composed of low-frequency components, the cut-off frequency was set to 500 Hz.

B. Polynomial Fit

Another technique for noise reduction is the polynomial fitting. This method consists of fitting a polynomial function to the signal data points, thereby smoothing out noise and revealing the underlying trend. Polynomial fitting is widely used in data analysis and signal processing, and is available in software packages such as MATLAB and Python's NumPy library.

A general polynomial of degree n can be expressed as:

$$P(x) = a_n x^n + a_{n-1} x^{n-1} + \cdots + a_2 x^2 + a_1 x + a_0 \tag{4}$$

A least squares fitting algorithm finds the best set of a_n coefficients that minimize the sum of the squared differences between the observed data points and the polynomial function.

C. The Single Diode Model

The SDM, better described at [14], [15] , is a widely adopted mathematical representation for photovoltaic cells and modules. It characterizes the current-voltage (I-V) behavior of a solar cell, accounting for the effects of temperature, irradiance, and other influencing factors. The model consists of a diode in parallel with a current source, which represents the photocurrent generated by the solar cell. The governing equation for the SDM is:

$$I = I_{ph} - I_0 \left(e^{\frac{(V+IR_s)}{nVth}} - 1 \right) - \frac{V + IR_s}{R_{sh}} \tag{5}$$

This transcendental equation describes the relationship between the output current I and the voltage V of a solar cell. Although it cannot be solved analytically for I, it can be addressed using numerical methods. For practical purposes, the equation can be expressed as in (6), where V is the independent variable and p is a vector containing the panel's parameters (constants):$\{I_{ph}, I_0, R_s, R_{sh}, nVth\}$.

$$I = f(V, p) \tag{6}$$

To obtain a more accurate voltage signal, an equation describing the solar panel's voltage as a function of its parameters, capacitance, and time is needed. Beginning with the continuous version of (1), (6) can be substituted into it, and the resulting ordinary differential equation (7) can then be numerically solved using methods such as the fourth-order Runge-Kutta algorithm [16]. Neglecting the voltage drop across the switch, the panel voltage is equal to the capacitor voltage, so $V = V_c$.

$$\frac{dV}{dt} = \frac{f(V, p)}{C} \tag{7}$$

The capacitor voltage V_c is obtained as the numerical solution of (7), which can be expressed as a function of time, capacitance C, and the parameter vector p.

$$V = f(t, C, p) \tag{8}$$

Using Equation 8, a least squares fitting algorithm is used to find an ideal set of parameters that best fits the function to the measured voltage data. The capacitor value and the time array are known, so the fitting process focuses on estimating the parameters of the SDM. With the estimated parameters, it is possible to calculate the current using (6).

IV. Results

This section presents the initial results obtained from applying the three described techniques. For each technique, the same raw data was used, which was gathered from a Jinko Solar panel, model JKM330PP-72. During the experiment, the irradiance measured 691 W/m^2, the ambient temperature was 28°C, and the panel temperature reached 54°C. All results

were comparable to the reference signal (in faded orange) measured by an oscilloscope.

To quantitatively evaluate the performance of each technique, the following statistical metrics were calculated between the processed current signal and the reference current signal: Mean Squared Error (MSE), Root Mean Squared Error (RMSE), Mean Absolute Error (MAE), and the coefficient of determination (R^2). For MSE, RMSE, and MAE, lower values indicate better performance, while for R^2, values closer to 1 indicate a better fit. The results are summarized in Table II.

For all techniques, the fitting of the voltage signal achieved a good fit(MSE < 0.07), therefore, they all produce a similar visual result, so the focus here is on the current signal, which is calculated using the processed voltage data.

TABLE II: Statistical Metrics for Signal Processing Techniques.

Method	**MSE**	**RMSE**	**MAE**	R^2
None (raw data)	0.704783	0.839514	0.628730	0.866849
Low-Pass Filter	0.093175	0.305247	0.253181	0.981802
Polynomial Fit	0.047191	0.217236	0.152251	0.990824
Single Diode Model	0.005762	0.075910	0.063273	0.998677

A. *Low-Pass Filter*

The low-pass filter was applied to the raw voltage data, and this refined data was used to estimate the current values, present in Figure 3 (a). When compared to the raw current (Figure 1 (b)), the filtered current signal presents a reduced noise level, which is proved by its lower statistical metrics, when compared to the raw current signal.

B. *Polynomial Fit*

In the Figure 4 (a), the current calculated using the fitted voltage data presents a smoother signal compared to the raw current data. However, it is important to note that the polynomial fitting technique (15th degree polynomial in this case) introduces distortion in the current signal, particularly in the regions near the open-circuit and short-circuit regions. While the distortion cannot be removed entirely, a higher polynomial degree is able to diminish it's effects with the cost of additional computing cost.

C. *Diode Model Fit*

The results of the SDM fitting are shown in Figure 5. The current calculated using the proposed method (Figure 5 (a)) is similar to the reference current signal, what is proven by its statistical metrics. In the data fitting process, the following parameters were estimated: $I_{ph} = 5.7644; I_0 = 2.9233e-08; R_s = 5.3082e-01; R_{sh} = 1.1292e+02; nVth = 1.0571$

V. Conclusion

This work presents results from three techniques used to improve the voltage signal obtained from a low-cost current sensorless curve tracer, where the current is calculated indirectly from the voltage data. The evaluated techniques include a digital low-pass filter, polynomial fitting, and a fitting to

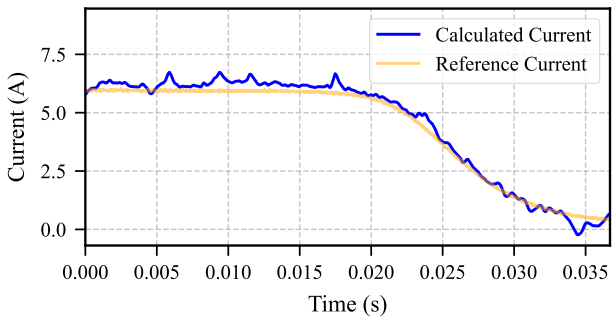

(a) Current × Time.

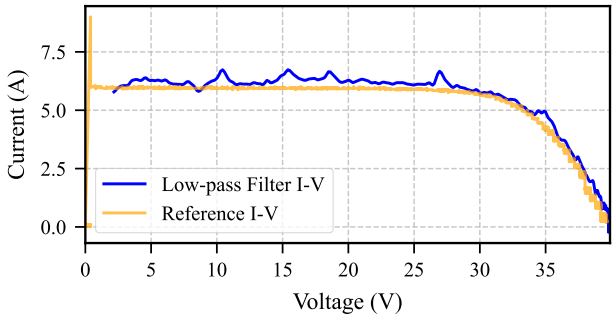

(b) Current × Voltage.

Fig. 3: Results of the low-pass filter. (a) Current calculated using the filtered voltage data; (b) I-V curve obtained from the filtered data.

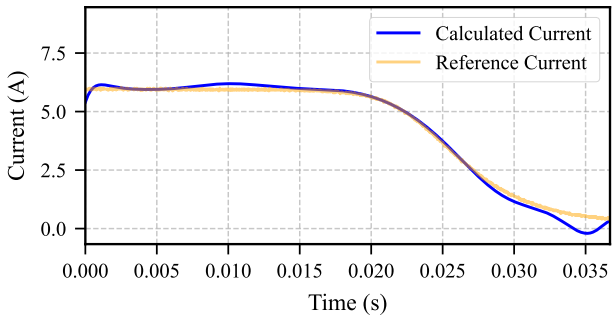

(a) Current × Time.

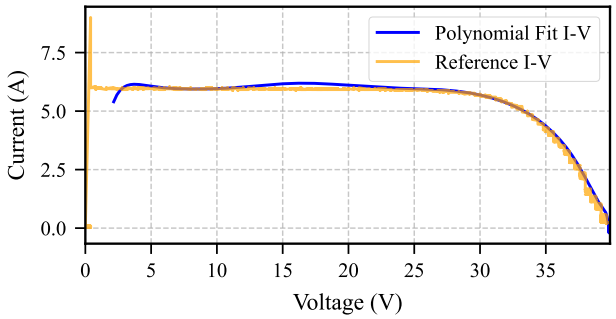

(b) Current × Voltage.

Fig. 4: Results of the polynomial fitting. (a) Current calculated using the fitted voltage data; (b) I-V curve obtained from the fitted data.

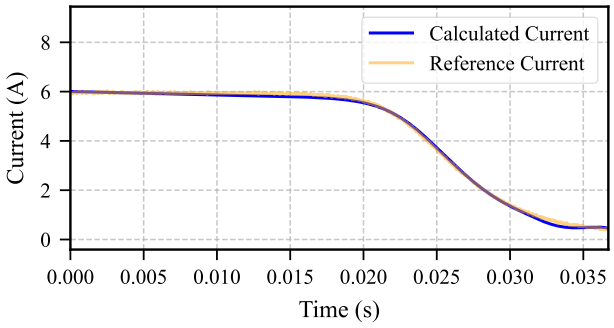

(a) Voltage × Current.

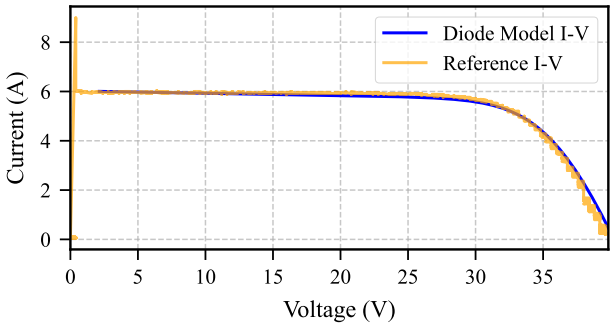

(b) Current × Voltage.

Fig. 5: Results of the single diode model fitting. (a) Current calculated using the fitted voltage data; (b) I-V curve obtained from the fitted data.

the single diode model (SDM). The results show that each method was capable of improving the current signal but with varying degrees of success. The low-pass filter is able to reduce the noise, although the output signal remains slightly affected by residual noise. The polynomial fitting technique smoothed the voltage signal but introduced distortion near the open-circuit and short-circuit regions. The curve fitting to the single diode model (SDM) provided a more accurate representation of the current signal, closely resembling the reference signal, but required greater computational resources. All results were validated by their statistical metrics, and the SDM fitting showed the best performance in terms of accuracy.

References

[1] Operador Nacional do Sistema Elétrico (ONS), "O sistema em números," 2025, https://www.ons.org.br/paginas/sobre-o-sin/o-sistema-em-numeros.

[2] ABSOLAR. (2025) Energia solar atinge 53 gw de capacidade instalada no brasil. Acessado em 22 de maio de 2025. [Online]. Available: https://www.absolar.org.br/noticia/https-canalsolar-com-br-energia-solar-capacidade-instalada-brasil-4/

[3] International Renewable Energy Agency (IRENA), "Renewable power generation costs in 2023," Abu Dhabi, 2024. [Online]. Available: https://www.irena.org/Publications/2024/Apr/Renewable-power-generation-costs-in-2023

[4] G. F. Nemet, "Interim monitoring of cost dynamics for publicly supported energy technologies," *Energy Policy*, vol. 37, no. 3, 2009.

[5] G. Ruddy, "Custo médio para instalar painéis solares cai no 1º tri com menor preço de matéria-prima," 2024, https://eixos.com.br/solar/custo-medio-para-instalar-paineis-solares-cai-no-1o-tri-com-menor-preco-de-materia-prima/.

[6] L. El Chaar, N. El Zein *et al.*, "Review of photovoltaic technologies," *Renewable and sustainable energy reviews*, vol. 15, no. 5, pp. 2165–2175, 2011.

[7] N. L. Chang, B. K. Newman, and R. J. Egan, "Future cost projections for photovoltaic module manufacturing using a bottom-up cost and uncertainty model," *Solar Energy Materials and Solar Cells*, vol. 237, p. 111529, 2022.

[8] L. G. T. Campos, V. P. Dardengo, D. d. C. Mendonça, E. M. d. S. Brito, A. F. Cupertino, and H. A. Pereira, "Desenvolvimento de um sistema traçador de curvas características de módulos fotovoltaicos com ajuste dinâmico," vol. 30, p. e202519, Feb. 2025. [Online]. Available: https://journal.sobraep.org.br/index.php/rep/article/view/1005

[9] M. De Riso, I. Matacena, P. Guerriero, and S. Daliento, "A wireless self-powered i-v curve tracer for on-line characterization of individual pv panels," *IEEE Transactions on Industrial Electronics*, vol. 71, no. 9, pp. 11 508–11 518, 2024.

[10] L. A. G. Lopes, D. C. d. Silva Junior, H. A. Pereira, V. Dardengo, A. F. Cupertino, and E. M. d. S. Brito, "Desenvolvimento de um caracterizador de módulos fotovoltaicos utilizando plataforma web," *XXV Congresso Brasileiro de Automática*.

[11] E. van Dyk, A. Gxasheka, and E. Meyer, "Monitoring current–voltage characteristics and energy output of silicon photovoltaic modules," *Renewable Energy*, 2005.

[12] S.-D. Ki, C.-W. Choi, J.-S. Ko, and D.-K. Kim, "Current-sensorless method for photovoltaic system using capacitor charging characteristics," *Energies*, vol. 17, no. 19, 2024. [Online]. Available: https://www.mdpi.com/1996-1073/17/19/4971

[13] GTracer, 2025. [Online]. Available: https://gtracer.gesep.com.br/

[14] V. M. Cavalcante Junior, T. A. Fernandes, R. A. Freitas, N. A. d. M. S. Amâncio, F. Bradaschia, and M. C. Cavalcanti, "Impact of optimization algorithm choice on nonlinear global model for photovoltaic energy generation forecasting," *Eletrônica de Potência*, vol. 29, Jun. 2024. [Online]. Available: https://journal.sobraep.org.br/index.php/rep/article/view/919

[15] M. G. Villalva, J. R. Gazoli, and E. R. F., "Modeling and circuit-based simulation of photovoltaic arrays," *Eletrônica de Potência*, vol. 14, no. 1, p. 35–45, Feb. 2009.

[16] S. C. Chapra, *Applied Numerical Methods with MATLAB: For Engineers and Scientists*, 3rd ed. McGraw-Hill Science/Engineering/Math, 2012.